A Novel Solar PV Inverter Topology Based on an LLC Resonant Converter

Necmi Altin[1,2], Saban Ozdemir[1,3], and Adel Nasiri[1]

[1] Center for Sustainable Electrical Energy Systems, University of Wisconsin-Milwaukee, WI, USA
[2] Department of Electrical and Electronics Engineering, Faculty of Technology, Gazi University, Ankara, Turkey
[3] Department of Energy Systems Engineering, Faculty of Technology, Gazi University, Ankara, Turkey
altin@uwm.edu; ozdemir@uwm.edu; nasiri@uwm.edu

***Abstract*— In this paper, a new topology for grid-connected solar PV inverter is proposed. The proposed topology employs an LLC resonant converter with high frequency isolation transformer in the DC-DC stage. The DC-DC converter stage is controlled to generate a rectified sine wave voltage and current at the line frequency. An unfolder inverter interfaces between this DC stage and the grid. Both phase-shift and frequency control methods are used to control the LLC resonant converter. The switching frequency is determined depending on the phase-shift angle to extend the zero-voltage switching (ZVS) region. The transformer leakage and magnetization inductances are also properly designed to provide ZVS for wide operation area. The LLC converter operates in the ZVS region except the narrow band around the zero-crossings of the inverter output current. Since the LLC resonant converter has a high frequency transformer, the line frequency transformer requirement is eliminated, and thus more compact and efficient design is obtained. The proposed topology is validated by the simulation and experimental results.**

Keywords—PV inverter, LLC resonant converter, phase-shift control, frequency modulation

I. INTRODUCTION

The voltage source inverters (VSIs) are commonly used in grid-connected inverter applications. Transformers have been an essential component of the grid connected VSI inverters to fulfill the voltage matching and isolation requirements [1]. Initial studies show that line frequency transformers (LFTs) are used at the output of the grid-connected voltage source inverters (VSIs) for this aim [2]. However, these transformers increase the cost, weight and size of the system and decrease its efficiency. Therefore, especially in low power applications such as micro-inverters or AC-module inverters, high frequency transformers (HFTs) embedded in DC-DC converter are used instead of the LFTs. This topology is also called high-frequency-link inverter. The topology with HFT is considered to be superior over the LFT one. In addition to providing the same advantages as the LFT, it also decreases the size and weight of the converter, and improves the overall efficiency of the system. In micro-inverters, several converter topologies and soft switching methods have been proposed for the DC-DC converter stage to improve the efficiency [3].

Isolated unidirectional or isolated bidirectional DC-DC converters have been commonly used and investigated for this inverter topology. Conventional phase-shift full-bridge (PSFB) converter provides galvanic isolation and zero-voltage-switching (ZVS) without any additional component. However, narrow ZVS range for the lagging leg and higher circulating current values especially for variable load conditions limits the improvements in power density and efficiency [4]. Dual active bridge (DAB) converters have become popular technology with their higher power capability, lower filter requirement, and ease of realizing soft-switching features [5]. The direction and amount of power can be easily controlled by controlling the phase-shift between the primary and secondary port voltages. However, this method results in higher circulating currents and narrows ZVS region. Although different modulation schemes have been proposed to overcome these problems; such as the trapezoidal and triangular modulation, these methods cannot resolve all the problems at once. Moreover, combining these modulation schemes make the control algorithm too complex with many parameters to handle [6].

The LLC resonant converters have been designed and used for different applications such as LED power supplies [7], battery chargers [8], [9], server power supplies, consumer electronics [10], and renewable energy systems [11]. They provide natural ZVS for primary side switches and zero-current-switching (ZCS) features [3]. In addition, circulating current of this converter can be controlled by proper design of the magnetizing inductor. The output voltage of the LLC resonant converter is a function of the switching frequency. Therefore, frequency modulation is commonly used in LLC converter applications. It can operate in buck mode and boost mode while being dependent on switching frequency. The phase-shift control is another control strategy applied to the LLC resonant converters. In this strategy, another gain which affect the input voltage amplitude is introduced and controlled in order to control the output voltage. Although it provides additional control degrees of freedom, the ZVS region and the analysis of the system are different from the frequency modulation case. Therefore, in the past studies, the phase-shift control method is generally applied to improve the startup or to keep the switching frequency constant at optimum value or in a limited range [12]-[14].

High frequency switching requirement of the VSI limits its applicable power and voltage levels. Nowadays, MV penetration of PV systems has become more common with the increasing power levels of the PV systems. However, in this high-frequency-link inverter topology, the isolated DC-DC converter is controlled to generate a DC voltage at the DC link and the VSI generates the AC output voltage and current.

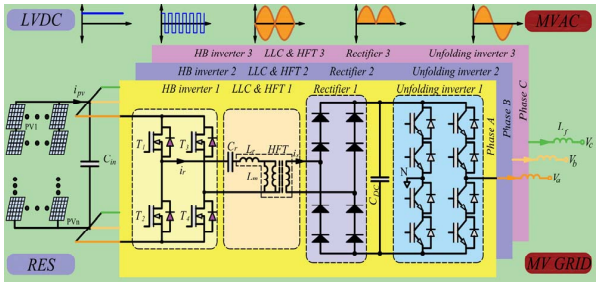

Fig. 1. Detailed topology of the proposed solar PV inverter.

The high-frequency-link inverters employing multilevel inverters have been also investigated to remove LFTs and increase the power density in medium voltage (MV) penetration of high power renewable energy plants. Different modular multilevel high frequency-link inverter topologies have been investigated because of the semiconductor switch voltage and current limitations [15], [16]. However, higher number of switches has negative effects on the reliability and efficiency of the system. In addition, the requirement of additional capacitors, inductors, complicated control schemes, and/or balancing circuits, makes the system more complex to deal with.

In this study, a high-frequency-link PV inverter topology is proposed to provide direct connection to the MV grid. The block diagram of the proposed inverter topology is given in Fig. 1. Here, the novelty from previous past studies, the isolated DC-DC converter is controlled to generate rectified sine wave voltage and current at the DC bus. The grid side inverter circuit operates at line frequency and only inverts the regulated DC voltage and current to AC. Thus, high frequency switching requirement at the grid side and related switching losses are removed. This makes the proposed system suitable for MV grid connected applications. All the current control and regulation actions are performed through the DC-DC converter stage. The LLC resonant converter is designed for this DC-DC converter stage. A hybrid modulation scheme employing both frequency modulation and phase-shift modulation methods is applied to control the current and to generate rectified sine waveform at the DC bus. Performance of the proposed topology and the control scheme are validated through MATLAB/Simulink simulations and experimental studies.

II. Proposed Solar PV Inverter

The proposed system suggests a novel topology where it provides direct connection to the MV grid which is essential in large scale PV systems. Basically, it employs three single-phase units where each unit consists of an unfolder inverter circuit and an LLC resonant converter as seen in Fig. 1. The LLC resonant converter itself composes of a full bridge inverter, a resonant capacitor, a low voltage (LV) to MV transformer and a full bridge diode rectifier. Here, the transformer is properly designed and additional resonant inductor requirement is removed. Thus, the LFT which is used to provide the voltage matching and galvanic isolation is replaced by the HFT which offers the same advantages with higher compactness and efficiency. The LLC resonant converter is controlled to generate a rectified sine wave voltage and current at the DC bus. The unfolder inverter inverts this signal to the AC by operating at line frequency,

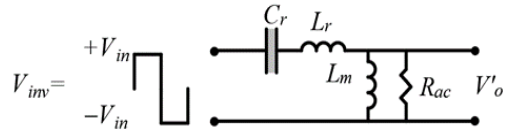

Fig. 2. Simplified model of the LLC converter.

and thus high frequency switching requirement at the MV stage is removed. This eases the high power MV converter design.

In Fig. 1, all the PV modules are connected to the three-phase inverter. Although this connection reduces the PV current ripple and makes the maximum power point (MPPT) tracking easier, PV modules can be organized to make three independent groups and can be connected to each phase of the inverter. Both buck and boost mode operations capability of the LLC resonant converter and single-phase based design of the system provides an extended MPPT range.

Main advantages of the proposed system can be summarized as: higher power density and efficiency. The proposed topology provides significant improvement in the total size and power density of the system by replacing the LFT with the compact HFT. In addition, this system proposes important efficiency improvements: 1) The natural ZVS and ZCS features of the LLC resonant converter helps in decreasing the switching losses. 2) Since the unfolder inverter operates at the line frequency, it has only conduction losses and removes the switching losses from the second stage of the system. 3) The HFT core size is directly related to the operating frequency; increasing the switching frequency decreases the core size and hence decreases the core losses. In addition, the LFT in conventional systems is continuously connected to the grid. This leads to power consumption in order to support the LFT core losses even if the PV system is not working. In the proposed system, since the transformer is part of the inverter, when the PV system is not working (e.g. at night), the transformer is not connected to the grid and it does not cause any power consumption.

A. The LLC Resonant Converter

During the last two decades, high efficiency and high power density requirements have led to an increase in the number of studies on LLC resonant converters. These converters are basically in serial resonance converter structures and widely used in isolated DC-DC converter applications. The equivalent circuit of the LLC converter stage can be illustrated as shown in Fig. 2 [17]. Here R_{ac} is the LLC converter load value which can be calculated as $R_{ac} = R_o 8n^2/\pi^2$, V_o' is the output voltage referred to the primary side, n is the turn ratio, L_m is magnetization inductance of the transformer, and finally, L_r and C_r are the series (resonant) capacitor and inductor, respectively. It is clear that different resonant tanks occur in the converter. When energy is being transferred from primary side to the secondary side, L_r and C_r resonate at a frequency given in (1) which is determined by the values of L_r and C_r and called as the first resonant frequency (f_{r1}):

$$f_{r1} = 1/\left(2\pi\sqrt{L_r C_r}\right) \tag{1}$$

When the transferred energy is zero, L_m and L_r are serial connected and resonate with the value of C_r. In this

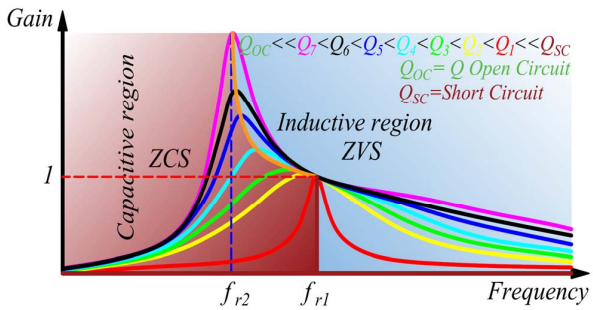

Fig. 3. Gain variation versus normalized frequency for different load values.

operation mode, a second resonant frequency given in (2) occurs:

$$f_{r2} = 1/\left(2\pi\sqrt{(L_r + L_m)C_r}\right) \tag{2}$$

A half bridge or full bridge inverter circuit is used to supply the resonant tank. When the switching signals are applied to the full bridge inverter which is the most commonly for high power applications, the generated resonant tank input voltage can be obtained as below:

$$v_{inv}(t) = \begin{cases} -V_{in}, & \frac{T}{2} \le t < 0 \\ V_{in}, & 0 \le t < \frac{T}{2} \end{cases} \tag{3}$$

Equation (3) can be written as in (4):

$$v_{inv}(t) = \sum_{k=1}^{\infty} \frac{4V_{in}}{k\pi} sin(k\omega_r t) \tag{4}$$

where ω_r is the angular resonant frequency.

Analyzing the LLC resonant converter is another subject to tackle. Four different analysis methods have been discussed in the literature. The First Harmonic Approximation (FHA) method is the most common method and provides acceptable accuracy for many applications [7]-[10]. It assumes that the power is transferred in the form of fundamental harmonic and the transformer secondary side current is always operating at critical conduction mode. Therefore, only fundamental harmonics of voltage and current are considered. By using FHA, the voltage equation can be obtained as below [17], [18]:

$$v_o'(t) = \frac{4V_{in}}{\pi} sin(\omega_r t) \tag{5}$$

The effect of the transformer magnetization inductance and load level determine which resonant frequency is dominant in the system. In other words, in a single switching period, in addition to the f_{r1}, the f_{r2} can be seen. The resonant tank impedance which has the major effect on the LLC resonant converter can be rewritten as in (6) by substituting variables:

$$z_{in} = \sqrt{L_r C_r}\left\{\left(\frac{f_n^2 Q}{L_n^2 + f_n^2 Q^2}\right) + j\left(\frac{f_n L_n}{L_n^2 + f_n^2 Q^2} - \frac{1 - f_n^2}{f_n}\right)\right\} \tag{6}$$

where f_n is the normalized frequency value given as $f_n = f_s/f_{r1}$, L_n is the normalized inductance value calculated as $L_n = \frac{L_r}{L_m}$, and Q is the Quality factor calculated as $Q = \frac{\sqrt{L_r/C_r}}{R_{ac}}$. It is clear from (6) that the switching frequency (f_s) which is determined by the designer, and the load value are two parameters that have major effect on the resonant tank impedance.

The voltage gain of the LLC resonant converter is dependent on the resonant tank parameters, switching frequency, and load. It can be expressed in (7) as:

$$M\big((Q, m, f_n)\big) = \frac{f_n^2(m-1)}{\sqrt{\left(mf_n^2 - 1\right)^2 + f_n^2\left(f_n^2 - 1\right)^2 (m-1)^2 Q^2}} \tag{7}$$

where $m = \frac{L_m + L_r}{L_r}$.

As seen from (5), once the LLC resonant converter is designed, the gain of the converter is only related to the load level and the switching frequency value. The variation of the converter gain versus the normalized frequency for different load conditions is depicted in Fig. 3. As can be seen from the figure, for $f_n < 1$, the converter gain is $M > 1$ and the LLC resonant converter operates in boost mode. If $f_n > 1$, meaning that the switching frequency is greater than the first resonant frequency, the converter gain is $M < 1$ and the LLC resonant converter operates in buck mode. Therefore, frequency modulation method which is based on changing the frequency to obtain appropriate gain is commonly applied to control the LLC resonant converters.

It is worth noting that the curves given in Fig. 3 are obtained for a specific *m* value. When *m* is changed, the gain characteristics of the converter also changes. Therefore, *m* value is another important factor which should be considered in our design stage. Lower *m* values will cause an increase in the maximum possible converter gain, narrowing the operating frequency range, and limiting the required maximum switching frequency value for a specific minimum gain. However, lower *m* values result in a higher circulating current (or reactive energy) and therefore, it increases the conduction losses and deteriorates the efficiency. Although larger *m* values help in limiting circulating current and conduction losses, the converter will suffer from higher maximum switching frequency value for the same attenuation level. In addition, the appropriate dead time value for the full bridge inverter switches in order to obtain ZVS is affected by the *m* value. The switch and parasitic capacitance C_{oss} should be discharged to obtain ZVS during the dead time. Larger *m* value decreases the actual current value during the dead time period. This may cause in losing ZVS operation and increase in power loss. Therefore, the *m* value, required maximum and minimum gain values, switching frequency band, switching losses, and determination of dead time should all be taken together into design consideration.

B. ZVS Analysis

In LLC resonant converters, there are two key factors that are effective in order to achieve ZVS. The first one is switching frequency. It is seen from Fig. 3 that the first and second resonant frequencies define three different operation regions. If f_s is higher than f_1, the converter operates in the first region. The impedance of the converter is inductive and therefore this region is called as inductive or buck region. If f_s is between f_1 and f_2 values, the converter operates in the

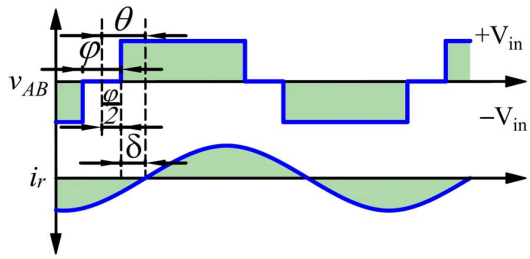

Fig. 4. The resonant tank current and input voltage.

second region. In this region, load value can introduce inductive or capacitive input inductance. When f_s is lower than f_1, the converter operates in the third region. Here, the input impedance is capacitive and thus it is called as capacitive region.

To achieve ZVS, the switch and parasitic capacitances should be discharged during the dead time. Lagging resonant current discharges the switch and parasitic capacitors and provides ZVS switching for the primary side switches [19], [20]. Therefore, it should be noted that the inductive resonant current is the first constraint in achieving ZVS operation. The impedance angle of the resonant tank defined in (8) can be written to be the first constraint of the ZVS:

$$\theta = arctan\left[-\frac{f_n^4Q^2+f_n^2L_n^2+f_n^2L_n-f_n^2Q^2-L_n^2}{f_n^3Q}\right] \quad (8)$$

The second constraint is related to the dead time and transformer magnetizing current. As mentioned above, the switch and parasitic capacitances should be discharged by the resonant tank current until the end of the dead time period. The resonant tank current is basically equal to the transformer magnetizing current during this interval [19]. Therefore, and in order to achieve ZVS operation, the magnetizing current should be high enough to discharge the capacitances during the dead time. However, higher magnetizing current values increase the circulating current and losses. Therefore, the dead time should be carefully determined according to the magnetizing inductance value as well as the switch and parasitic capacitances values. Once this constraint is fulfilled, the ZVS condition can be easily simplified to $\theta>0$. It is worth noting that keeping f_s larger than f_1 guarantees the operation in this condition.

However, this is only valid for frequency modulation condition. When the phase-shift control is applied, even if f_s is higher than f_1 and the input impedance of the resonant tank is inductive, the zero intervals at the inverter voltage may cause losing the ZVS mode. As seen in Fig. 4, while the impedance angle is θ, the actual angle between the zero-crossings of the voltage and the current is δ. Therefore a new angle, called ZVS angle (δ), should be determined to investigate the ZVS condition as below:

$$\delta = \begin{cases} \theta & for \quad \varphi = 0 \\ \theta - \frac{\varphi}{2} & for \quad 0 < \varphi \leq \pi \end{cases} \quad (9)$$

Here, φ is the phase-shift angle applied to control the converter gain. It is clear that to guarantee the ZVS, δ has to be positive. Therefore, the ZVS constraint is modified as $\delta>0$ for phase-shift control.

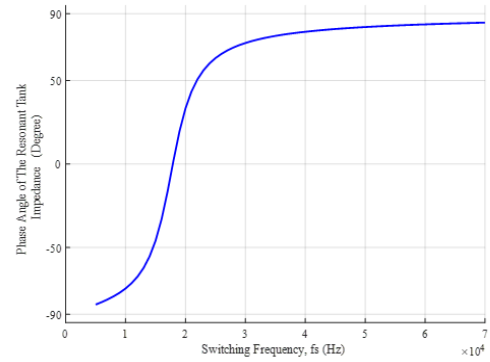

Fig. 5. Phase angle variation of the resonant tank impedance versus switching frequency.

III. The Control Scheme Of The Proposed System

In this study, the LLC resonant converter is employed in grid-connected inverter as given in Fig. 1. Thus, the voltage gain of the LLC converter has to be reduced down to zero. This is practically impossible with only switching frequency control. Therefore, the phase-shift control is employed. In this control method, a phase-shift (φ) is added between two legs of the inverter. Thus, the fundamental component of the resonant tank supply voltage given in (10) will be dependent to the phase-shift angle.

$$v_{AB1} = \frac{4}{\pi} sin\frac{\pi-\varphi}{2} sin(2\pi f_s t), \ 0 \leq \varphi \leq \pi \quad (10)$$

The inductive resonant tank impedance is one of the constraints that have to be fulfilled in order to achieve ZVS operation. For a traditional LLC resonant converter, this condition is fulfilled if the switching frequency is higher than the resonant frequency. However, as discussed in the previous section and in case of phase-shift control, the constraint should be modified. Higher phase-shift angle may cause leading resonant current which means capacitive mode operation even when the switching frequency is higher than the resonant frequency value. The resonant tank impedance angle and the phase-shift angle are two parameters which define the operation zone as inductive or capacitive mode.

Since the phase-shift angle has to be controlled from 0 to π, achieving ZVS across the entire operation area is theoretically impossible. The ZVS operation range depends on the angle of the resonant tank impedance; higher values of the impedance angle provide wider ZVS operation range. As it is seen from (4) that, higher m value enables this. However, increasing L_m may also cause losing ZVS. Therefore, L_m and t_d should be selected carefully. Although selecting a constant and higher switching frequency can be used to extend the ZVS region, the switching frequency in

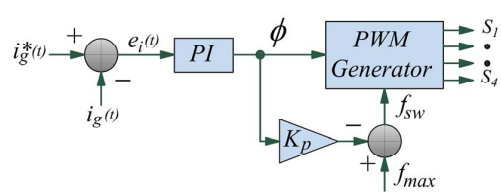

Fig. 6. Block diagram of the proposed control scheme.

TABLE I. SYSTEM PARAMETERS

Symbol	Value
Resonant inductor, L_r	10μH
Resonant capacitor, C_r	4μF
Magnetizing inductor, L_n	250μH
Transformer turm ratio, n	1:1.1
Switching frequency, f_s	30-60kHz.
Supply voltage, V_{in}	200V
Grid voltage and frequency, U_g, f_g	120V, 50Hz
DC buc capacitance, C_{inv}	1.2μF

this study is controlled according to the phase-shift angle in order to provide wider ZVS range. The variation of impedance angle versus switching frequency is given in Fig. 5. A proportional (P) controller is employed to calculate the switching frequency depending on the phase-shift value.

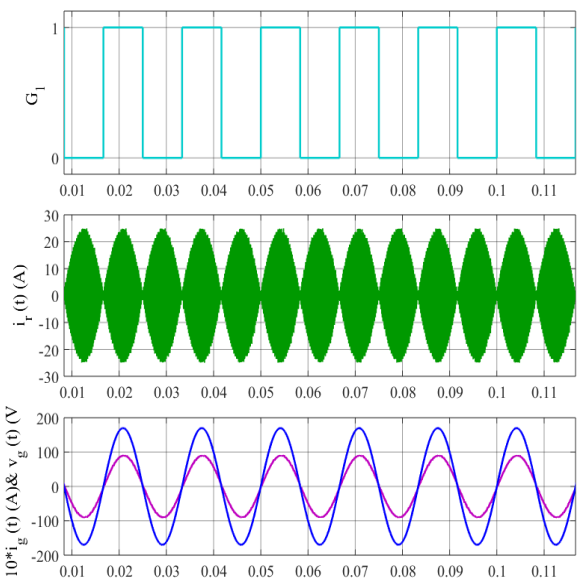

(a)

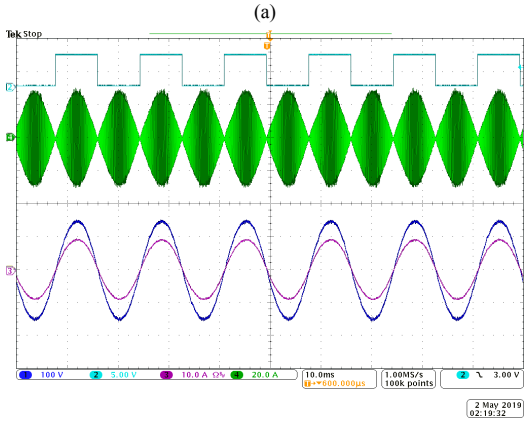

(b)

Fig. 7. The grid voltage, grid current and resonant current waveforms (a) Simulation, (b) Experiment (Ch.1 is the grid voltage (100V/div), Ch. 3 is the grid current (10A/div), Ch. 4 is the resonant current (20A/div)

In the proposed operation, the switching frequency value is close to the resonant frequency at high current with lower phase-shift angle. However, the switching frequency is increased when the phase-shift increases to track the decreasing reference current signal for each half cycle of the reference output current signal. Thus, the ZVS operation range is extended and average value of the switching frequency is decreased, and thus more efficient operation is obtained. The block diagram of the proposed control scheme is depicted in Fig. 6. It is seen that there are two control variables; the switching frequency and the phase-shift angle. The phase-shift angle is calculated according to current error by the PI controller. The output of the PI controller can be expressed as below:

$$\varphi(t) = K_P\,[i_g(t) - i_g(t)^*] + K_I \int [i_g(t) - i_g(t)^*]dt \quad (11)$$

where $i_g(t)$ is the system output current injected to the grid and $i_g(t)^*$ is its reference signal. Thus, the phase-shift angle is determined and the switching frequency is calculated via the P controller.

IV. SIMULATION AND EXPERIMENTAL RESULTS

The validation of the proposed LLC resonant converter based inverter is performed by simulation and experimental studies. The proposed system is modelled with MATLAB/Simulink. The evaluation of the input signals, control actions and PWM generation were implemented using Altera FPGA. The analog signals were read by AD7328 ADC chips, LA-55P current sensors and resistive voltage dividers. The main parameters of the system are given in Table 1.

In Fig. 7 (a) and (b), the simulated and experimental waveforms of the switching signal for one switch of the unfolder inverter circuit, the resonant current, the grid voltage and the grid current are given. It is seen that the proposed system can regulate the resonant current to generate the sinusoidal output current. The output current is in sinusoidal waveform with very limited harmonic contents. Thus, the proposed system can meet the conditions declared in international standards like IEC61727 and IEEE1547.

The dynamic performance of the proposed topology and controller is also investigated. An abrupt change is applied to the reference current signal where the value is increased from 40% to 100%. The obtained simulation and experimental results are given in Fig. 8. In this figure, switching signal for a switch of the high frequency inverter, the resonant current, the DC bus current and the grid voltage are shown. The proposed controller controls the phase-shift and switching frequency value to track the reference current signal. It is seen from both simulation and experimental results that the proposed system provides good dynamic response and does not cause any oscillations or overshoot. As it is mentioned previously, achieving ZVS for the whole operation range is impossible, but by modulating the switching frequency, the ZVS region can be extended with lower average switching frequency. This in turn will lead to a more efficient operation. The proposed topology employs a high-frequency transformer and it can provide galvanic isolation and voltage matching that are required for MV connection. Thus, LFT requirement can be eliminated and more compact and efficient MV PV system can be obtained.

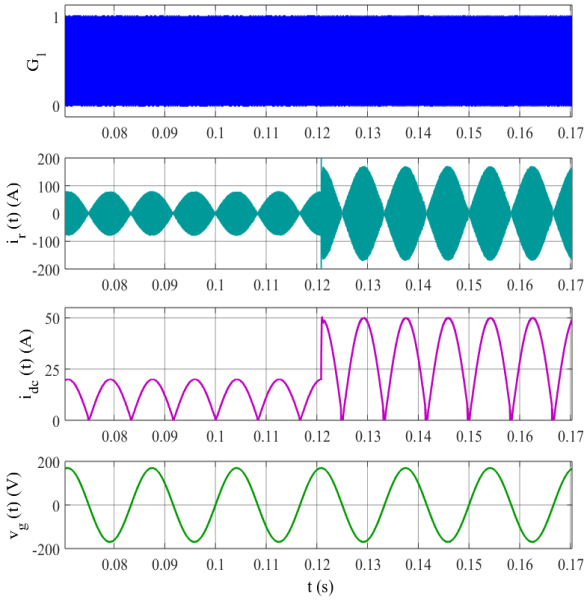

(a)

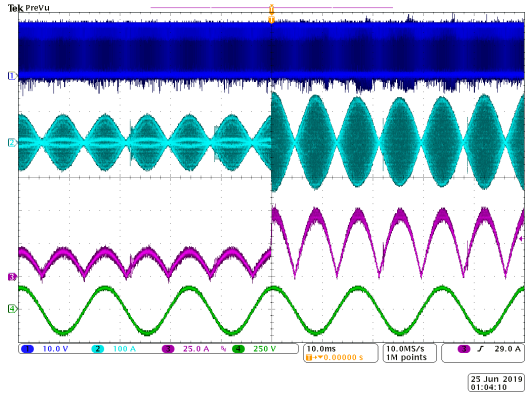

(b)

Fig. 8. The grid voltage, DC bus current and resonant current waveforms at reference change (a) Simulation, (b) Experiment (Ch.2 is the resonant current (100A/div) Ch. 3 is the DC bus current (25A/div), Ch. 4 is the grid.

V. Conclusion

In this study, high-frequency DC link inverter topology is introduced to provide direct MV connection. The proposed system employs the LLC resonant converter and unfolder inverter. The LLC resonant converter is used to regulate the sinusoidal output current of the grid connected inverter. Then the unfolder inverter which is operating at line frequency inverts this regulated current to the AC. The ZVS conditions and constraints which are different from the conventional LLC resonant converters with frequency modulation are explained. Phase-shift and frequency controls are employed side by side to control the current and provide extended ZVS region. By using controlled switching frequency, the average switching frequency and the corresponding switching losses are decreased as compared to the constant and higher switching frequency providing the same ZVS region. A PI controller is employed to control the converter output current and calculate the phase-shift value.

A PI controller is employed to control the converter output current and calculate the phase-shift value. A P controller is used to determine the switching frequency according to the phase-shift angle. It is seen from both simulation and experimental results that the proposed system successfully generates sinusoidal current and injects it to the grid. The current contains less harmonic components and meets the international standards. It is shown that the proposed control system employing phase-shift control and frequency control schemes provide fast response and good dynamic behavior. It is also seen that ZVS operation range is extended by both proper transformer design and controlled switching frequency.

Acknowledgment

This material is based upon work supported by the National Science Foundation under Grant No. 1650470 for GRAPES I/UCRC center. Any opinions, findings, and conclusions or recommendations expressed in this material are those of the author(s) and do not necessarily reflect the views of the National Science Foundation. Dr. Necmi Altin and Dr. Saban Ozdemir thank the financial support which they received from the Scientific and Technological Research Council of Turkey (TUBITAK) BIDEB-2219 Postdoctoral Research program.

References

[1] I. Sefa, and N. Altin, Grid interactive photovoltaic inverters - A review. Journal of the Faculty of Engineering and Architecture of Gazi University, vol. 24, pp. 409-424. 2009.

[2] I. Sefa, S. Ozdemir, H. Komurcugil, and N. Altin, “An enhanced lyapunov-function based control scheme for three-phase grid-tied VSI with LCL filter,” IEEE Transactions on Sustainable Energy, vol. 10, no.2, pp. 504-513, April 2019.

[3] L. Chen, A. Amirahmadi, Q. Zhang, N. Kutkut, and I. Batarseh, “Design and implementation of three-phase two-stage grid-connected module integrated converter,” IEEE Transactions on Power Electronics, vol. 29, no. 8, pp. 3881–3892, Aug 2014.

[4] I.-O. Lee and G.-W. Moon, “Analysis and design of phase-shifted dual H-bridge converter with a wide ZVS range and reduced output filter,” IEEE Trans. Ind. Electron., vol. 60, no. 10, pp. 4415–4426, Oct. 2013.

[5] B. Zhao, Q. Song, W. Liu, and Y. Sun, “Overview of dual-active-bridge isolated bidirectional dc–dc converter for high-frequency-link powerconversion system,” IEEE Transactions on Power Electronics, vol. 29, no. 8, pp. 4091–4106, Aug 2014.

[6] Y. Cho, W. Cha, J. Kwon, and B. Kwon, “High-efficiency bidirectional dab inverter using a novel hybrid modulation for stand-alone power generating system with low input voltage,” IEEE Transactions on Power Electronics, vol. 31, no. 6, pp. 4138–4147, June 2016.

[7] I. Demirel and B. Erkmen, “A very low-profile dual output LLC resonant converter for LCD/LED TV applications,” IEEE Trans. Power Electron., vol. 29, no. 7, pp. 3514–3524, Jul. 2014.

[8] Y. Wei, N. Altin, Q. Luo and A. Nasiri, "A High Efficiency, Decoupled On-board Battery Charger with Magnetic Control,"2018 7th International Conference on Renewable Energy Research and Applications (ICRERA), Paris, 2018, pp. 920-925.

[9] Y. Wei, Q. Luo, X. Du, N. Altin, A. Nasiri, and J. M. Alonso, “A Dual Half-bridge LLC Resonant Converter with Magnetic Control for Battery Charger Application”, IEEE Transactions on Power Electronics, DOI: 10.1109/TPEL.2019.2922991.

[10] G. Li, J. Xia, K. Wang, Y. Deng, X. He and Y. Wang, "Hybrid Modulation of Parallel-Series LLC Resonant Converter and Phase Shift Full-Bridge Converter for a Dual-Output DC–DC Converter," in IEEE Journal of Emerging and Selected Topics in Power Electronics, vol. 7, no. 2, pp. 833-842, June 2019.

[11] S. M. Tayebi, H. Hu, S. Abdel-Rahman and I. Batarseh, "Dual-Input Single-Resonant Tank LLC Converter with Phase Shift Control for

PV Applications," in IEEE Transactions on Industry Applications, vol. 55, no. 2, pp. 1729-1739, March-April 2019.

[12] D. Yang, C. Chen, S. Duan, J. Cai and L. Xiao, "A variable duty cycle soft startup strategy for LLC series resonant converter based on optimal current-limiting curve," IEEE Transactions on Power Electronics, vol. 31, no. 11, pp. 7996-8006, Nov. 2016.

[13] J. Kim, C. Kim, J. Kim, J. Lee and G. Moon, "Analysis on load-adaptive phase-shift control for high efficiency full-bridge LLC resonant converter under light-load conditions," IEEE Transactions on Power Electronics, vol. 31, no. 7, pp. 4942-4955, July 2016.

[14] E. S. Kim, J. Lee, Y. Heo and T. Marius, "LLC resonant converter with wide output voltage control ranges operating at a constant switching frequency", IEEE Applied Power Electronics Conference and Exposition, pp. 2124-2128, 2018.

[15] Y. Shi, R. Li, Y. Xue, and H. Li, "High-frequency-link-based gridtied pv system with small dc-link capacitor and low-frequency ripplefree maximum power point tracking," IEEE Transactions on Power Electronics, vol. 31, no. 1, pp. 328–339, Jan 2016.

[16] M. R. Islam, Y. Guo and J. Zhu, "A High-Frequency Link Multilevel Cascaded Medium-Voltage Converter for Direct Grid Integration of Renewable Energy Systems," in IEEE Transactions on Power Electronics, vol. 29, no. 8, pp. 4167-4182, Aug. 2014.

[17] J. Deng, S. Li, S. Hu, C. C. Mi, and R. Ma, "Design methodology of LLC resonant converters for electric vehicle battery chargers," IEEE Trans. Veh. Technol., vol. 63, no. 4, pp. 1581–1592, May 2014.

[18] M. Rashidi, M. Sabbah, A. Bani-Ahmed, A.l Nasiri, and M. H. Balali. "Design and implementation of a series resonant solid state transformer." Energy Conversion Congress and Exposition (ECCE), pp. 1282-1287. IEEE, 2017.

[19] R. Ren, B. Liu, E. A. Jones, F. Wang, Z. Zhang, and D. Costinett, "Accurate zvs boundary in high switching frequency llc converter," in 2016 IEEE Energy Conversion Congress and Exposition (ECCE), Sept 2016, pp. 1–6.

[20] S. M. S. I. Shakib and S. Mekhilef, "A frequency adaptive phase shift modulation control based llc series resonant converter for wide input voltage applications," IEEE Transactions on Power Electronics, vol. 32, no. 11, pp. 8360–8370, Nov 2017.